XVIII International Conference on Water Resources
CMWR 2010
J. Carrera (Ed)
CIMNE, Barcelona 2010

A CHANNEL NETWOK MODEL AS A FRAMEWORK FOR CHARACTERIZING VARIABLY-SATURATED FLOWS IN BIOFILM-AFFECTED SOILS: CONCEPTUAL MODEL

Ravid Rosenzweig, Alex Furman and Uri Shavit

Civil and Environmental Engineering,
Technion IIT, Haifa 32000, Israel
e-mails: rravid@technion.ac.il , afurman@technion.ac.il, aguri@technion.ac.il

Key words: hydraulic properties; biofilm; pore network

1 INTRODUCTION

Modeling flow and transport in biofilm-affected soils is a subject of growing interest which emerged from the understanding that microbial populations, in particular biofilms, play a key role in the fate and transport of contaminants in the subsurface. Although numerous works have tried to model the flow and transport under saturated conditions[1-3], only a few dealt with the unsaturated environment[4, 5].

The common practice for describing the flow in saturated and unsaturated soils is by using macroscopic flow equations in which the knowledge of the microscale soil geometry is not directly required. Although the macroscopic approach was proven to be very efficient for many problems, macroscopic models of biofilm-affected medium yielded inconclusive results when verified against experiments[2]. Thus, in cases where biofilm growth changes the microscopic structure of the soil, a model that specifying the microscopic structure of the soil-pores is needed.

Recently we have performed a preliminary analysis of the influence of biofilm distribution on the soil unsaturated conductivity function[6]. In this work we used the classic capillary tube model to represent the soil pores (i.e., the pores are simulated as a bundle of capillary tubes of different diameters). The analysis showed that the biofilm spatial distribution within the pore space has a significant effect on the hydraulic properties of the soil. Although the capillary model is widely used and is easy to obtain, it has a few shortcomings, primarily the over-simplistic assumption regarding the binary nature of the pores (i.e., each pore is either completely water-filled or completely empty under a prescribed matric head). Moreover, the lack of pores connectivity and the unrealistic cylindrical geometry of the capillaries further reduce the model efficiency in determining soil hydraulic properties[7]. The lack of pore connectivity can be especially significant when dealing with biofilms. Thullner et al.[1, 2] showed that under saturated conditions, modeling the pores as one-dimensional capillary tubes could not reproduce connectivity-related effects. These effects, such as flow bypasses generated from preferential biofilm growth were demonstrated in experiments and were successfully reproduced using pore-network models.

Or and Tuller[7] suggested to model the soil-pores by using channels having a triangular cross-section. The channels can be either water-filled (for saturated flow) or partially-filled

(for unsaturated flow), where the water-filled fraction is related to the matric head through the curvature of the water surface. Or and Tuller[7] solved the flow in a bundle of channels but didn't take into account the channels connectivity. In this work we expand Or and Tuller's[7] concept and propose a framework in which the soil pores are simulated as a network of channels having a triangular cross-section. The representation of the soil pores by a network of triangular channels is superior to the capillary model in two aspects. It eliminates the binary (full/empty) behavior and takes into account inter-pore connectivity. The presented modeling framework can serve as a first step in simulating the combined water flow, solute transport and biofilm growth under variably saturated conditions.

2 CONCEPTUAL MODEL

2.1 Water retention

Following Or and Tuller[7], we consider a channel with a triangular cross-section as outlined in Fig. 1. The channel length is *L*, its height is *H*, and the spanning angle is γ. In their paper Or and Tuller[7] considered water retention caused by both capillary forces and adsorbed water films. It was shown that the contribution of the adsorbed water films is dominant under dry conditions, while under wet conditions capillary forces dominate. Since the aim of our proposed model is to describe flow of water in biofilm-affected soils, and since biofilm contribution is significant under wet conditions, we chose to ignore the adsorbed water film and consider water retention by capillary forces alone. Under unsaturated condition the matric head is related to the radius of the water surface curvature by the Young-Laplace relationship, $r(h)=-\sigma/\rho g h$, with r being the radius of curvature, σ the surface tension, h is the matric head, ρ the density, and g the gravitational acceleration. The water-filled cross-sectional area A increases with the matric head as follows,

$$A = r^2(h)\left[\frac{1}{\tan(\gamma/2)} - \frac{\pi(180-\gamma)}{360}\right] \tag{1}$$

The channel saturation equals one for $h \geq h_{max}$ and A/A_f for $h < h_{max}$, where A_f is the total cross-sectional area of the channel ($A_f = H^2 \tan(\gamma/2)$) and h_{max} is a critical head in which the water surface reaches the top-edge of the channel. Following Or and Tuller[7], we assume that for $h > h_{max}$ the entire channel cross-section is filled with water. The relation between h_{max} and the channel dimensions are given by,

$$h_{max} = -\frac{\sigma\cos(\gamma/2)}{\rho g H \tan(\gamma/2)} \tag{2}$$

The total water retention of the channel network can now be obtained by calculating the volume-weighted average of the water retention of the individual channels. We note that the water retention of the channel network is independent of the channels arrangement (network topology). This is in contrast to other flow-related properties, such as the hydraulic

conductivity, which are highly dependent on the channels arrangement within the network.

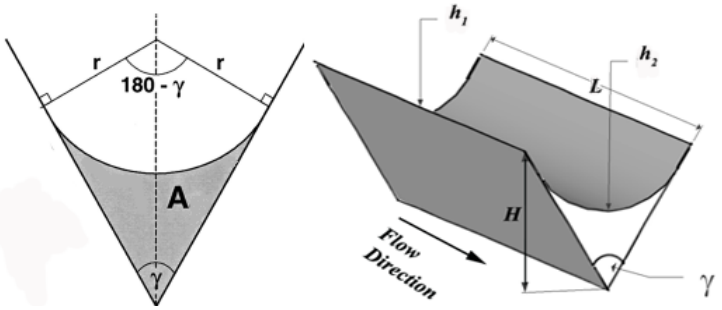

Figure 1:A cross section and a 3D illustration of the channel and water surface configuration (after Or and Tuller[7]).

2.2 The flow solution in an unsaturated channel

The flow within the channel is solved by considering the following assumptions: (a) the flow regime is laminar with a small Reynolds-number and therefore the inertia terms are negligible; (b) the velocity is unidirectional and fully developed; (c) the water surface is stable (i.e. its shape is determined by the matric head and not by the flow); and (d) the channel orientation is horizontal such that the flow is driven only by matric head gradients.

For the unsaturated case, in which the channel is partially occupied by water, we use the results of Ransohoff and Radke[8] who solved the flow of water retained in corners by capillary forces. Ransohoff and Radke[8] solved numerically the two-dimensional Stokes equation and derived the following expression for the average velocity,

$$\bar{v} = -\frac{r^2(h)}{\eta_0 \varepsilon}\rho g \frac{\partial h}{\partial l} = -\frac{\sigma^2}{\rho g \eta_0 \varepsilon h^2}\frac{\partial h}{\partial l} \tag{3}$$

where l is the coordinate in the direction of the channel axis, η_0 is the dynamic viscosity, $\bar{v}$ the axial velocity, and ε is a flow resistance factor which is dependant on the channel spanning angle and given by,

$$\varepsilon = \exp\left(\frac{b + d\gamma}{1 + c\gamma}\right) \tag{4}$$

with b=2.124, c=-0.00415, d=0.00783 and γ is in the range of $10^0 < \gamma < 150^0$. By multiplying the average velocity by the cross-sectional area and and solving along the channel length, the channel flow rate is expressed in terms of the matric heads at the channel edges,

$$Q_u = \frac{\chi}{3L}\left[\frac{1}{h_2^3} - \frac{1}{h_1^3}\right]; \quad \chi = \frac{1}{\eta_0 \varepsilon}\frac{\sigma^4}{(\rho g)^3}\left[\frac{1}{\tan(\gamma/2)} - \frac{\pi(180-\gamma)}{360}\right] \tag{5}$$

h_1 and h_2 are the matric heads at the channel inlet and outlet, respectively. Substituting $\Phi = h^{-3}$, we obtain the following linear equation for the flow rate,

$$Q_u = \frac{\chi}{3L}\left[\Phi_2 - \Phi_1\right] \tag{6}$$

2.3 The flow solution in a saturated channel

For saturated flow the average cross-sectional velocity is calculated by substituting the maximum radius of curvature $r_{max} = H\tan(\gamma/2)/\cos(\gamma/2)$ (when the water surface touches the channel top edges) into Eq. (3),

$$\bar{v} = -\frac{H^2\tan^2(\gamma/2)\rho g}{\eta_0 \varepsilon \cos^2(\gamma/2)}\frac{\partial h}{\partial l} \tag{7}$$

The flow rate for the saturated case is then obtained by multiplying Eq. (7) by the full cross-sectional area A_f,

$$Q_s = -\frac{H^4\tan^3(\gamma/2)\rho g}{\eta_0 \varepsilon \cos^2(\gamma/2)}\frac{\partial h}{\partial l} \tag{8}$$

To bring Eq. (8) into a similar form as Eq. (6), we use the transformation $dh = -d\Phi h^4/3$ to obtain,

$$Q_s = -\frac{\chi_2 h^4}{3}\frac{\partial \Phi}{\partial l}; \qquad \chi_2 = -\frac{H^4\tan^3(\gamma/2)\rho g}{\eta_0 \varepsilon \cos^2(\gamma/2)} \tag{9}$$

The approximated solution of equation (9) is obtained by linearization,

$$Q_s \approx \frac{\chi_2 h^{*4}}{3}\left[\Phi_2 - \Phi_1\right] \tag{10}$$

with $h^* = (h_1 + h_2)/2$.

2.4 The transition between saturated to unsaturated flow conditions

For a variably saturated system, transition between saturated and unsaturated conditions may occur within a channel. One way to treat the transition is by splitting the channel into two parts accordingly. However, this may lead to increased computational effort since the split location has to be found iteratively. Instead, we apply here a more simple approach by using the following general scheme,

$$Q = S_c \cdot Q_s + (1 - S_c)\cdot Q_u \tag{11}$$

where Q_u is the unsaturated flow rate (Eq. 5), Q_s is the saturated flow rate (Eq. 10) and S_c is the saturated fraction of the channel. S_c equals zero for unsaturated channels, one for saturated channels and for partially saturated channels (in which h_{max} lies between h_1 and h_2) is approximated by a linear interpolation, i.e. $S_c = \left(max(h, h_2) - h_{max}\right)/(h_1 - h_2)$. Although Eq.

(11) is an approximated solution of the channel flow rate, it creates a smooth transition between the saturated and unsaturated flows. Moreover, for large networks the error in using the outlined scheme when calculating the flow rate is expected to be limited as the absolute differences between h_1 and h_2 decreases.

2.5 Network solution

A two-dimensional pore network was assembled by arranging the channels in a square lattice, with each node connecting four channels. For simplicity, it was assumed that the nodes have no volume. In the following we use a uniform length for all the channels; however the square arrangement doesn't prohibit assigning variable channel lengths, allowing representation of the medium's tortuosity.

The flow rate and head distributions within the network are obtained by solving Eqs. (6) and (10) for the unsaturated and saturated flow respectively, while satisfying a mass balance at each of the nodes. The solution consists of an iterative procedure, in which (a) an initial solution is assumed; (b) the equations of saturated flow are linearized (Eq. 10); (c) the resultant system of linear equations is solved for Φ; (d) the heads at the nodes are updated; and (e) the saturated equations are relinearized using the updated heads. Steps (c)-(e) are repeated until the change between results of consecutive iterations is smaller than a certain threshold. In all simulations presented here Dirichlet boundary conditions (constant heads h_{in} and h_{out}) were assumed on the two opposite sides of the rectangular domain, while no-flow condition was assigned on the remaining two boundaries.

2.6 Upscaling and calibration

Soil representation by a network of channels is obtained by assigning size distributions for the channel geometrical properties. Following Or and Tuller[7] the channels heights were assumed to distribute according to a gamma distribution,

$$f(H,\zeta,\omega)=\frac{H^{\zeta-1}}{\Gamma(\zeta)\omega^{\zeta}}exp\left(-\frac{H}{\omega}\right) \tag{12}$$

where ω and ζ are the scale and shape parameters of the gamma distribution and Γ is the gamma function. In order to obtain closed form expressions, Or and Tuller[7] chose to use ζ =3 and keep the spanning angle γ constant. We followed Or and Tuller[7] by using ζ =3 but allowed more flexibility, by assuming that γ has a truncated normal distribution with $10^o<\gamma<150^o$,

$$f(\gamma,\mu,\sigma_n)=\frac{1}{\sqrt{2\pi\sigma_n^{\,2}}}exp\left(-(\gamma-\mu)^2/\left(2\sigma_n^{\,2}\right)\right) \tag{13}$$

where μ and σ_n are the mean and the standard deviation of the normal distribution.

The parameters of the gamma and normal distribution (ω, μ, and σ_n) were obtained by fitting the water retention curve (WRC) of the network to known WRCs of common soils.

The optimization problem was solved by the genetic algorithm toolbox of MATLAB (Mathworks) by minimizing the differences between the network-obtained and known WRCs.

3. RESULTS

The applicability of the model was evaluated by considering homogeneous networks, consisting of uniform channels and by heterogeneous networks in which the geometrical parameters were allowed to vary according to Eqs. (12-13).

3.1 Homogeneous network

A rectangular homogeneous network was constructed from 4,900 channels (50 by 50 nodes). The flow within the network was solved using the outlined scheme, obtaining the heads in each node. As a result of the assigned boundary conditions and our choice of a uniform network, flow exists only in the channels that are aligned along the streamwise direction (X), while the water in the perpendicular channels is stagnant. Figure 2a displays the head profiles along the streamwise direction for h_{in} = -0.01 m, h_{out} = -0.2 m, L= 0.0204 m (such that the entire network length equals 1m), H = 0.001 m and two γ values (30^0 and 60^0). The transition from saturated to unsaturated flow is marked in the figure and is evident in the shape of the head profiles. Whereas under saturated conditions the head exhibits a linear behavior, the transition to unsaturated regime changes the shape of the head profile, causes it to drop sharply near the outlet boundary, as expected from the -3 power in Eq. (5).

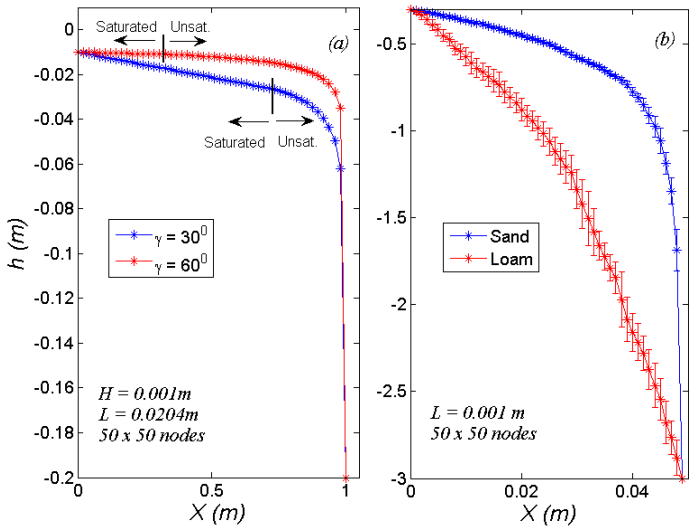

Figure 2: Head profiles in (a) homogeneous network for two spanning angles (h_{max} = -0.0265m and -0.011 m for $\gamma = 30^0$ and 60^0, respectively) and (b) in heterogeneous networks , representing sand and loam .

3.2 Heterogeneous networks

To obtain a representation of a soil pore space, heterogeneous networks of 50 by 50 nodes (4,900 channels) were used. The statistical distributions of H and γ were determined by Eqs.

(12) and (13) respectively where ω, μ, and σ_n were fitted to obtain the best match to the WRCs of sand and loam taken from the soil catalogue of Carsel and Parrish[9] (specified in terms of the van Genuchten's[10] parameters n and α). Table 1 lists the van Genuchten's parameters of the WRCs of the two soils and the ω, μ, and σ_n values obtained by the genetic algorithm. Figure 3 presents the original WRCs of Carsel and Parrish[9] alongside the fitted WRCs obtained from the channel network. It can be seen that the sand exhibits a better match to the "real" WRCs while for the loam the fitted WRC deviates from that of Carsel and Parrish[9], especially in the high and low saturation ranges. It is possible that other distributions for H and γ will provide a better fit. A search for such distributions is underway and is expected to improve our results.

Soil	n	α [m^{-1}]	ω·E7 [m]	μ	σ_n
Sand	2.68	14.5	3	149.7	2.95
Loam	1.56	3.6	3.59	121.2	62.53

Table 1: Properties of the van-Genuchten relation[10] taken from Carsel and Parrish[9] and fitted distribution parameters.

Figure 2b depicts the mean head distribution (averaged over the spanwise direction, Y) along the streamwise direction for the heterogeneous networks whose geometrical properties were outlined above and for h_{in} = -0.3 m, h_{out} = -3 m and L= 0.001 m. The difference between the profiles shape is evident. While the head profile of the sand drops steeply, the loam exhibits a much moderate behavior. This is related to the pore-size distribution of the two soils. The close-to-uniform pore size distribution of the sand leads to a steep decline in the head profile, similarly to that obtained for the homogeneous network. On the other hand, the graded pore-size distribution of the loam results in the moderate decline shown in Fig. 2b.

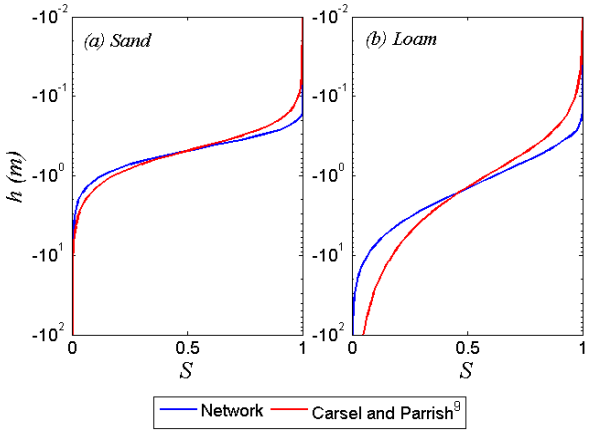

Figure 3: Fitted WRCs obtained from the network compared with the original WRCs form Carsel and Parrish[9]. (a) Sand, (b) Loam.

4 SUMMARY AND CONCLUSIONS

In the current work we presented a channel network as a tool to simulate variably-saturated flows. The concept is based on channels having a triangular cross-section, whose water-filled fraction is dependent on the matric potential. The flow within the network is solved by computing the flow rate at each channel (accounting for saturated and unsaturated conditions) and by maintaining a mass balance at each of the network nodes. The applicability of the model was demonstrated using homogeneous networks and heterogeneous networks in which the WRCs of the network was fitted to WRCs of real soils by finding the correct statistical distribution of the channels' geometrical properties. As the new model explicitly specifies the pores microstructure, it serves studies of biofilm affected soils through modeling the coupled water flow, solute transport and biofilm growth problem under variably-saturated conditions.

ACKNOWLEDGMENT

We would like to acknowledge the Star-Gilbert Memorial Fund and the Eshkol Fund of the Israeli ministry of science and technology for their generous financial support.

REFERENCES

[1] M. Thullner, J. Zeyer, and W. Kinzelbach, "Influence of microbial growth on hydraulic properties of pore networks," *Transport in Porous Media,* 49, pp. 99-122, Oct 2002.

[2] M. Thullner, M. H. Schroth, J. Zeyer, and W. Kinzelbach, "Modeling of a microbial growth experiment with bioclogging in a two-dimensional saturated porous media flow field," *Journal of Contaminant Hydrology,* 70, pp. 37-62, May 2004.

[3] S. W. Taylor and P. R. Jaffe, "Biofilm Growth and the Related Changes in the Physical-Properties of a Porous-Medium .1. Experimental Investigation," *Water Resources Research,* 26, pp. 2153-2159, Sep 1990.

[4] R. R. Yarwood, M. L. Rockhold, M. R. Niemet, J. S. Selker, and P. J. Bottomley, "Impact of microbial growth on water flow and solute transport in unsaturated porous media," *Water Resources Research,* 42, Oct 2006.

[5] M. Mostafa and P. J. Van Geel, "Conceptual models and simulations for biological clogging in unsaturated soils," *Vadose Zone Journal,* 6, pp. 175-185, Feb 2007.

[6] R. Rosenzweig, U. Shavit, and A. Furman, "The Influence of Biofilm Spatial Distribution Scenarios on Hydraulic Conductivity of Unsaturated Soils," *Vadose Zone Journal,* 8, pp. 1080-1084, Nov 2009.

[7] D. Or and M. Tuller, "Flow in unsaturated fractured porous media: Hydraulic conductivity of rough surfaces," *Water Resources Research,* 36, pp. 1165-1177, May 2000.

[8] T. C. Ransohoff and C. J. Radke, "Laminar-Flow of a Wetting Liquid Along the Corners of a Predominantly Gas-Occupied Noncircular Pore," *Journal of Colloid and Interface Science,* 121, pp. 392-401, Feb 1988.

[9] R. F. Carsel and R. S. Parrish, "Developing Joint Probability-Distributions of Soil-Water Retention Characteristics," *Water Resources Research,* 24, pp. 755-769, May 1988.

[10] M. T. van Genuchten, "A closed-form equation for predicting the hydraulic conductivity of unsaturated soils," *Soil Science Society of America Journal,* 44, pp. 892-898, 1980.